Why Hour Glasses Tick

X-l. Wu and K. J. Måløy*
Department of Physics and Astronomy, University of Pittsburgh, Pittsburgh, Pennsylvania 15260

A. Hansen, M. Ammi, and D. Bideau
Group Matière Condensée et Matériaux, Université de Rennes 1, F-35042 Rennes Cedex, France
(Received 13 April 1993)

We have found experimentally that the flow of sand in an hour glass is oscillatory in a certain range of parameters. The oscillatory motion results from a coupling between the flow of sand and convection of air through the sand matrix. The period of the oscillation is remarkably insensitive to the grain size, while the mass of the sand contained in one period strongly depends on it.

PACS numbers: 46.10.+z, 62.20.−x, 62.40.+i

Despite its long history of investigation, the flow of granular materials, such as sand and powders, still remains poorly understood [1,2]. This is partly caused by the granular state being a singular state of matter, neither liquid nor solid. The behavior of sand in an hour glass is a good example of this. In commercial hour glasses, the sand flows continuously as a liquid, but the discharge is nearly constant during the flow. The remarkable stability of the flow is a result of "arching" effects which produce a tenuous force network, rendering the pressure throughout the sand nearly constant. This is to be contrasted to a liquid, where the pressure changes continuously with height. In this Letter, we demonstrate another surprising effect: When the grain size is small, ~ 10–100 μm, continuous flow is only found in a narrow range of the dimensionless parameter R/r, where r is the radius of a sand grain and R is the radius of the orifice (see Fig. 1), namely, $2 < R/r < 12$. For large particles, $R/r \sim 2$, the flow is discontinuous due to formation of stable arches in the orifice. For small particles, $R/r > 12$, the flow is intermittent with a well-defined temporal frequency. In this intermittent regime, the system exhibits an extraordinary sensitivity to external noise, temperature change, and interparticle interactions. This regime is caused by complex interactions between the pressure of the gas (air) present in the hour glass and the pressure caused by the mechanical contacts within the sand.

The oscillatory phenomenon reported in this Letter is new. However, that the coupling between the motion of grains and the interstitial fluid—in this case air—may profoundly affect the granular flow has been known for a long time in the engineering community [3,4]. Sometimes this coupling has dramatic consequences such as the case when several thousand tons of cement powder poured out of a silo in Germany, covering the whole plant area—after which it started to rain [5]. This accident was caused by air trapped inside the cement powder thus causing it to fluidize. Another effect caused by the same mechanism is the dependence of the angle of repose on the ambient air pressure [4].

The hour-glass oscillation shows several intriguing properties that might deepen our understanding of granular flow in the regime where the interstitial fluid is important, i.e., the flow of fine powders. We mention here the most striking of these properties. *The period of the oscillation seems independent of the size of the particles.* This result is all the more remarkable when taking into account the complex nature of the mechanism behind the oscillation, relying both on the mechanical properties of the grains and on the hydrodynamics of the interstitial fluid.

It is a surprise that there is such a strong coupling between the flow properties of the sand and the air in the hour glass. Usually, the relative importance of the behavior of the two phases, sand and air, on the overall behavior of the combined system is expressed through the *Bagnold* number, $B =$ (viscous drag forces)/(mechanical forces caused by the other grains), which we simply estimate as $9\eta v/2r^2 g\rho$, i.e., the ratio between the drag force on a single particle and its weight. Here, η is the viscosity of air, r is the radius of the sand grains, g is the gravitational constant, ρ is the mass density of the sand, and v is the relative velocity between the gas and the grains. As we will show later, the Bagnold number [2,6] for the hour glass in the intermittent regime is of the order of 10^{-3}. From this estimate, it is clear that the mechanism generating the intermittent behavior is not caused by viscous drag on single particles. However, what does cause this

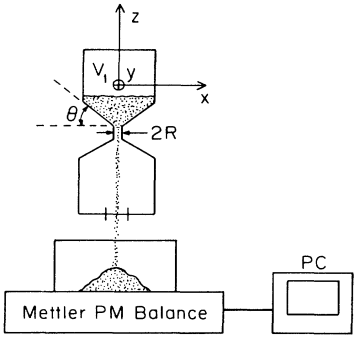

FIG. 1. The experimental setup.

0031-9007/93/71(9)/1363(4)$06.00

behavior is a pressure gradient in the air created by the emptying of the upper chamber by the falling sand, which is strong enough to stabilize the sand—thus hindering more sand from falling. The pressure difference is of the order of 10^{-4} atm and thus very small. Indeed, sealing the lower chamber of the hour glass (see Fig. 1) and simply holding it, thus slightly warming the lower chamber, is enough to stop the flow entirely. That this small pressure difference is sufficient to stabilize the sand is again caused by arching effects in the sand.

Our experimental apparatus is illustrated in Fig. 1. The relevant dimensions of the hour glass are as follows: The radius R of the orifice is 0.1 cm, the slope of the shoulder is $\theta \simeq 45°$, and the volume of the two chambers is $V_1 = V_2 = 200$ ml. To facilitate weight measurements, the lower chamber is open to the atmosphere, while the upper chamber is closed. Because of the conic shape above the orifice, the pressure drop is localized in a small region, $\sim R^3$. As a result, the overall flow behavior is insensitive to the particular construction of the hour glass, such as the length of the neck and the slope of the shoulder. In a typical experiment, the initial weight of the sand—in reality glass beads—was ~ 10 g, occupying a small fraction of V_1. Cleaned and dried glass beads, with uniform diameters $d = 41$, 58, 81, 115, and 160 μm, falling out of the hour glass were collected by a cup and weighted by a Mettler balance. The balance had a sampling rate ~ 7 Hz and was interfaced to a computer. To achieve good statistics, several thousand avalanches were measured and the cumulative mass (M) was recorded by the computer.

As mentioned, for $R < 2r$, the flow is discontinuous, due to the formation of stable arches in the orifice. For $R > 12r$, the flow is also discontinuous, giving rise to intermittent avalanches whose size is a strong function of the dimensionless parameter R/r. Associated with the intermittent flow, we observed "air bubbles" propagating upward through the bead packing above the orifice, somewhat resembling density waves observed in hoppers [7].

Figure 2 shows the mass $M(t)$ of the glass beads that have fallen onto the balance as a function of time for samples with $d = 41$ and 81 μm. We note that, on large time scales, the rate of mass transfer $\Delta M/\Delta t$ is almost a constant and increases markedly as d increases. On small time scales, however, the flow is discontinuous and appears to have a reasonably well-defined period T. The discontinuity in the mass transfer is a manifestation of the avalanches. Careful inspection of the time traces reveals that within each period T there are two different phases, the active phase T_a (transient regime, where the sand flows) and the inactive phase T_i (plateau regime, where the sand stops flowing), with $T = T_a + T_i$. For small beads, the active phases are much shorter than the inactive phases, resulting in sharp steps in the time trace. For large beads, however, the difference between the two phases vanishes. This flow behavior persists throughout the entire measurement; it is independent of the height of the bead packing in the upper chamber, suggesting that the dynamics is localized in a small region near the orifice.

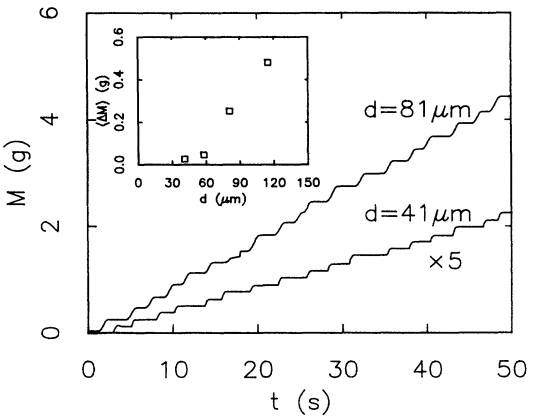

FIG. 2. Time sequence of mass transfer $M(t)$. The measurements are for glass beads with $d = 41$ and 81 μm. The data for $d = 41$ μm have been multiplied by a factor of 5 in order to bring them to the same scale as the other set of data. The oscillatory motion gives rise to an active phase, during which M increases sharply, and an inactive phase, during which M remains constant. The inset shows the average mass transfer, $\langle \Delta M \rangle$, *per* avalanche as a function of d.

Changing the diameter of the beads by merely a factor of 2 leads to a change of the average mass transfer $\langle \Delta M \rangle$ per avalanche as large as a factor of 10 in certain cases, as shown in the inset of Fig. 2. This sensitivity is confirmed by studying the cumulative mass distribution function $N(\Delta M > \Delta M^*)$ for avalanches of size ΔM, as shown in Fig. 3. Here the measurements were conducted for four bead sizes, $d = 41$, 58, 81, and 115 μm. Accompanying the increase in $\langle \Delta M \rangle$, the distribution function

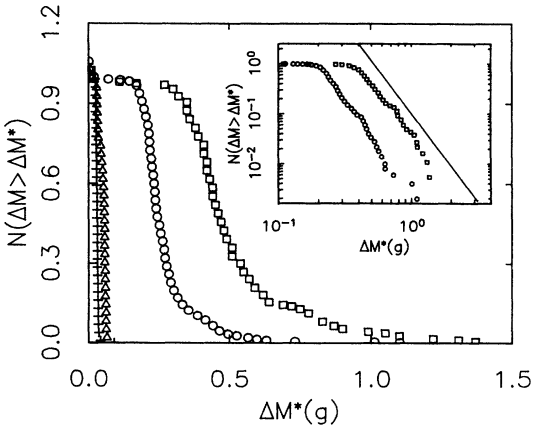

FIG. 3. Cumulative mass distribution $N(\Delta M > \Delta M^*)$. The measurements are for $d = 41$ (crosses), 58 (triangles), 81 (circles), and 115 μm (squares), respectively. The inset is a log-log plot of $N(\Delta M > \Delta M^*)$ for beads with $d = 81$ (circles) and 115 μm (squares). The solid line, having a slope of -3.5, is a guide to the eye.

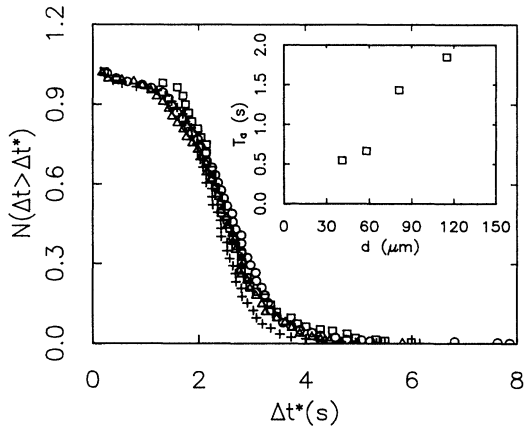

FIG. 4. Cumulative time distribution $N(\Delta t > \Delta t^*)$. The measurements are for $d = 41$ (crosses), 58 (triangles), 81 (circles), and 115 μm (squares), respectively. Despite different d, the distribution functions are quantitatively the same for all the beads. The inset shows the duration of the active phase T_a vs d.

appears to be broadened as evidenced by the long tail in $N(\Delta M > \Delta M^*)$. The inset of Fig. 3 shows a log-log plot of $N(\Delta M > \Delta M^*)$ vs ΔM for two large bead sizes, $d = 81$ and 115 μm. Asymptotically, $N(\Delta M > \Delta M^*)$ is consistent with a power law, $\Delta M^{-3.5}$, as shown by the solid line.

Having analyzed the mass distribution of avalanches, we now turn our attention to the temporal behavior of the avalanches. Figure 4 shows the cumulative time distribution function $N(\Delta t > \Delta t^*)$ for the same set of glass beads. This function essentially measures the time interval Δt between the avalanches. Despite the large noise seen in the data, we note that the functional form of $N(\Delta t > \Delta t^*)$ is nearly the same for all the samples. Furthermore, the average time interval, which is identical to the period of the avalanche $\langle \Delta t \rangle \equiv T$, turns out to be also the same, $T \simeq 2.5$ s, for all the samples [8]. The dynamics exhibit certain complexities that are not well understood. Notably, the duration of the active and the inactive phases appears to depend on d, with T_a increasing almost linearly with d, as shown in the inset of Fig. 4. For the largest beads ($d = 115$ μm) that still exhibit oscillatory motion, T_i approaches zero while T_a becomes comparable to the period T. For beads slightly larger than 115 μm, the flow is continuous. It is intriguing that the transition from the intermittent to the continuous flow regimes occurs smoothly and the period T is robust, independent of the particle size.

To qualitatively interpret the above observations, consider the hour glass as shown in Fig. 1. When an avalanche of size ΔM occurs, the free volume in the upper chamber expands slightly, resulting in a small change in air density ρ_1 in that chamber,

$$\Delta\rho_1 = -\rho_2 \Delta M / \rho_g \phi V_1 , \tag{1}$$

where ρ_2 is the air density in the lower (open) chamber, $\rho_g (\approx 2.5$ g/cm$^3)$ is the density of the glass, and ϕ is the volume fraction of the glass beads, which is assumed to be a random close packing with $\phi \approx 0.64$ [1]. For an isothermal process the change in ρ_1 is accompanied by a drop in the pressure ΔP_1 which can be calculated using the ideal gas law, $\Delta P_1 = N_0 k_B \Theta \Delta\rho_1 / \overline{M}$, where k_B is the Boltzmann constant, N_0 is the Avogadro's constant, Θ is the absolute temperature, and $\overline{M}$ is the average molar weight of the gas. Assuming that the flux of glass beads is constant during the avalanche, the time derivative of ΔP_1,

$$\frac{d\Delta P_1}{dt} = \frac{N_0 k_B \Theta}{\overline{M}} \frac{d\Delta\rho_1}{dt} , \tag{2}$$

must also be constant; i.e., the pressure P_1 in the upper chamber decreases linearly in time during the active period T_a. However, when the avalanche ends, the pressure P_1 will start increasing since the bead packing is permeable to the air flow. The rate of change of air density in the upper chamber is related to the air current q passing through the orifice set up by the pressure difference between the two chambers,

$$\frac{d\Delta\rho_1}{dt} = \frac{\rho_2 q}{V_1} . \tag{3}$$

The air flux may further be related to the difference in air pressure across the bead packing through the Darcy equation [1],

$$q = -(\kappa\pi R/\eta)\Delta P_1 , \tag{4}$$

where κ is the permeability of the bead packing and η is the viscosity of the air. In deriving Eq. (4) we noted that the conic shape of the orifice ensures that the pressure gradient is localized in a small region, $\sim R^3$, and hence the proper length scale appearing in the Darcy equation is R. Combining Eqs. (2), (3), and (4), we obtain

$$\frac{d\Delta P_1}{dt} = -\frac{P_2 \pi \kappa R}{\eta V_1} \Delta P_1 . \tag{5}$$

Integrating this equation yields

$$\Delta P_1(t) = \Delta P_1^{\max} e^{-t/\tau} , \tag{6}$$

with the characteristic time for the pressure relaxation being

$$\tau = \eta V_1 / P_2 \pi \kappa R . \tag{7}$$

Thus, in the inactive phase, the pressure difference in the upper chamber vanishes exponentially. We may estimate τ for the bead packing that we have used. The permeability κ varies between 1.5×10^{-8} and 1.2×10^{-7} cm^2 for the bead diameters we have used [9]. The viscosity of air is 2×10^{-4} P and P_2 is 1 atm. This leads to τ being in the range from 1 to 10 s, the longer times being associated with the smaller beads. The $\Delta P_1^{\max}$ is the pressure in the upper chamber at the point when the bead packing stabilizes. Likewise, there will be a minimum pressure

difference, $\Delta P_{\downarrow}^{\min}$, at which the beads start flowing again. We can relate $\Delta P_{\downarrow}^{\max}$ and $\Delta P_{\downarrow}^{\min}$ to the size of an avalanche ΔM through Eq. (1),

$$\Delta P_{\downarrow}^{\max} - \Delta P_{\downarrow}^{\min} = P_2 \Delta M / \rho_g \phi V_1 , \quad (8)$$

and the inactive period T_i,

$$\Delta P_{\downarrow}^{\min} = \Delta P_{\downarrow}^{\max} e^{-T_i/\tau} . \quad (9)$$

What phenomenon is responsible for the existence of $\Delta P_{\downarrow}^{\min}$ and $\Delta P_{\downarrow}^{\max}$? Gravity acts downward on the bead packing, creating an internal pressure in the glass beads. But because of the presence of arching, this pressure is essentially independent of the depth of the packing. The magnitude of the pressure is proportional to the weight of a cluster of beads residing in a volume ξ^3, shielded by an arch. Here the "correlation length" ξ, *the size of a typical arch,* is of the order of 10 and 10^2 bead diameters [10]. To give a rough estimate of the magnitude of the pressures involved, we find about 10^{-4} atm when ξ is ~ 10 bead diameters. Because of the presence of the active and inactive phases, we expect there to be two correlation lengths ξ_a and ξ_i associated with the two phases. In the active phase, the moving particles cause the bead packing to dilate, resulting in fewer contacts between the grains and, hence, greater average arch size $\xi_a (> \xi_i)$. Thus, the internal pressure during the active phase is greater than the internal pressure during the inactive phase.

We may at this stage estimate the Bagnold number B as defined in the beginning of this paper. Using the Darcy equation (4) with a pressure difference of 10^{-4} atm we find that the air velocity at the orifice is ~ 1 cm/s. This leads to $B \approx 10^{-3}$ for the smallest beads, $d = 41$ μm; for larger beads B will be even smaller. Thus, the hydrodynamic drag on individual particles is insignificant for the dynamics of avalanches.

As soon as the air pressure in the upper chamber drops below that of the lower chamber, there will be a force on the bead packing in the upward direction. This will counteract the internal pressure in the bead packing due to gravity. Suppose that the air pressure gradient is large enough to stabilize the system; we estimate that in order to create an air pressure difference of $\sim 10^{-4}$ atm in the packing of $d = 41$ μm, an avalanche should contain approximately 0.05 g of beads. This is indeed comparable to the observed values reported in Fig. 3. Once the bead packing is stabilized, the air pressure difference diminishes exponentially, until it reaches the level of the inactive internal pressure, i.e., $\Delta P_{\downarrow}^{\min} = \rho_g \phi g \xi_i$. The beads will then start flowing, and, as a result, the air pressure gradient increases again. As the packing is now moving, we need a *larger* air pressure gradient to counteract the larger internal pressure of the moving packing. When they balance, $\Delta P_{\downarrow}^{\max} = \rho_g \phi g \xi_a$, the bead packing stops flowing, and the cycle then repeats.

We may estimate ξ_i and ξ_a from the data shown in Figs. 3 and 4. For $d = 58$ and 81 μm, the corresponding pressure relaxation times are $\tau = 4$ and 2 s. Using the measured period, $T = 2.5$ s, and the data in the inset of Fig. 4 we found that $T_i = 1.8$ and 1.0 s for $d = 58$ and 81 μm, respectively. Thus, in all the cases, the ratio T_i/τ is about 0.5. Using Eq. (9) and the relation between the pressure and the correlation length we found that ξ_a/ξ_i is approximately 1.6. Finally, from Eq. (8) and the data in Fig. 3 we estimate ξ_a/d to be ~ 60 and 250, and ξ_i/d to be ~ 30 and 100, respectively. These length scales are reasonable compared to those measured in photoelastic experiments [10].

Our observation is contrary to the common belief that the oscillatory motion and the accompanying density waves result solely from the arching of glass beads in the orifice. In fact it is not difficult to qualitatively test our theory by opening the cap on the upper chamber. In this case the pressure in both chambers will be the same (atmospheric pressure) and the flow should be continuous. This is indeed what has been observed. Our preliminary measurements also indicated that the oscillation period T can be regulated by the average pressure P in the hour glass, with T (or T_a) increasing as P decreases, in qualitative agreement with our prediction. Unlike that of the continuous flow regime, the flow in the intermittent regime is very sensitive to external noises, such as vibrations and air convections. The effects of the external noise on the flow behavior in the hour glass will be reported elsewhere.

Måløy and Wu acknowledge hospitality and financial support from University of Rennes 1. Ammi, Bideau, and Hansen acknowledge support from the GdR CNRS "Physique des Milieux Hétèrogènes Complexes." Groupe Matière Condensée et Materiaux is CNRS URA804.

*Permanent address: Fysisk Institutt, Universitetet i Oslo, N-0316 Oslo 3, Norway.

[1] *Disorder and Granular Media,* edited by D. Bideau and A. Hansen (North-Holland, Amsterdam, 1993).
[2] H. M. Jaeger and S. R. Nagel, Science **255**, 1523 (1992).
[3] W. Bruff and A. W. Jenkine, Powder Technol. **1**, 252 (1967).
[4] R. M. Nedderman, *Statics and Kinematics of Granular Materials* (Cambridge Univ. Press, Cambridge, 1991).
[5] W. Bruff, Teknisk Ukeblad **41**, 737 (1967) (in Norwegian).
[6] R. A. Bagnold, *The Physics of Blown Sand and Desert Dunes* (Methuen, London, 1941); R. A. Bagnold, Proc. R. Soc. London A **25**, 49 (1954).
[7] G. W. Baxter *et al.*, Phys. Rev. Lett. **62**, 2825 (1989).
[8] A slight shift in the period T was observed for unbaked glass beads, presumably due to moisture that alters the particle-particle interaction.
[9] E. Guyon, L. Oger, and T. J. Plona, J. Phys. D **20**, 1637 (1987).
[10] E. Guyon *et al.*, Rep. Prog. Phys. **53**, 373 (1990).